



# A Combined Experimental–Theoretical Study on Diels-Alder Reaction with Bio-Based Furfural: Towards Renewable Aromatics

Ivan Scodeller, Karine de Oliveira Vigier, Eric Muller, Chengming Ma, Frédéric Guégan, Raphael Wischert, François Jerome

## ► To cite this version:

Ivan Scodeller, Karine de Oliveira Vigier, Eric Muller, Chengming Ma, Frédéric Guégan, et al.. A Combined Experimental–Theoretical Study on Diels-Alder Reaction with Bio-Based Furfural: Towards Renewable Aromatics. ChemSusChem, 2020, 10.1002/cssc.202002111 . hal-03015071

**HAL Id: hal-03015071**

**<https://hal.science/hal-03015071>**

Submitted on 19 Nov 2020

**HAL** is a multi-disciplinary open access archive for the deposit and dissemination of scientific research documents, whether they are published or not. The documents may come from teaching and research institutions in France or abroad, or from public or private research centers.

L'archive ouverte pluridisciplinaire **HAL**, est destinée au dépôt et à la diffusion de documents scientifiques de niveau recherche, publiés ou non, émanant des établissements d'enseignement et de recherche français ou étrangers, des laboratoires publics ou privés.

# A combined experimental-theoretical study on Diels-Alder reaction with bio-based furfural: towards renewable aromatics

Dr. Ivan Scodeller,<sup>[a]</sup> Prof. Karine De Oliveira Vigier,<sup>[a]</sup> Dr. Eric Muller,<sup>[b]</sup> Dr. Changru Ma,<sup>[c]</sup> Dr. Frédéric Guégan,<sup>[a]\*</sup> Dr. Raphael Wischert,<sup>[c]\*</sup> and Dr. François Jérôme<sup>[a]\*</sup>

Dedicated to P.H. Dixneuf for his outstanding contribution to catalysis

[a] Institut de Chimie des Milieux et Matériaux de Poitiers, CNRS, Université de Poitiers, 1 rue Marcel Doré, 86073 Poitiers (France)..

E-mail: [francois.jerome@univ-poitiers.fr](mailto:francois.jerome@univ-poitiers.fr), [frederic.quegan@univ-poitiers.fr](mailto:frederic.quegan@univ-poitiers.fr).

[b] Centre de Recherche Solvay, 85 Avenue des Frères Perret, 69190 Saint-Fons (France).

[c] Eco-Efficient Products and Processes Laboratory, UMI 3464 CNRS/Solvay, 3966 Jin Du Road, Xinzhuang, Industrial Zone, Shanghai 201108 (China). E-Mail: [raphael.wischert@solvay.com](mailto:raphael.wischert@solvay.com).

Supporting information for this article is given via a link at the end of the document

**Abstract:** We investigate the synthesis of relevant renewable aromatics from bio-based furfural derivatives and cheap alkenes, through a Diels-Alder/aromatization sequence. The prediction and the control of the *ortho* : *meta* selectivity in the Diels-Alder step is an important issue to pave the way to a wide range of relevant renewable aromatics, but it remains a challenging task. Through a combined experimental-theoretical approach, we reveal that, as a general trend, *ortho*- and *meta* cycloadducts are the kinetic and thermodynamic products, respectively. The nature of substituents, both on the dienes and dienophiles, significantly impacts the feasibility of the reaction, through a modulation on the nucleo- and electrophilicity of the reagents, as well as the *ortho* : *meta* ratio. We show that the *ortho* : *meta* selectivity at the reaction equilibrium stems from a subtle interplay between charge interactions, favoring the *ortho* products, and steric interactions, favoring the *meta* isomers. This work also points towards a path to optimize the aromatization step.

## Introduction

The production of aromatics, such as Benzene, Toluene and Xylene (BTX) represent an enormous market, with 45 million tons of benzene produced per year, for instance.<sup>[1]</sup> A myriad of valuable downstream aromatic chemicals can be obtained from BTX, such as terephthalic acid, cyclohexane, cumene, phenol, and styrene, to mention a few only. Industrially, BTX are mainly produced by catalytic reforming of naphtha or steam cracking of hydrocarbons. With the exponential increase of the world population, chemistry will face difficulty to supply aromatics in the future and alternative routes are nowadays explored. In this context, there is a growing interest in the synthesis of aromatics from biomass.<sup>[2]</sup>

A wide range of aromatics can be theoretically obtained from lignocellulosic biomass. For instance, alkyl phenols can be produced by the catalytic lignin-first depolymerization process<sup>[3]</sup> or from tannins present in lignocellulosic biomass.<sup>[4]</sup> Aromatics can be also produced from hemicellulose or cellulose through the furfural<sup>[5-13]</sup> or 5-hydroxymethylfurfural platform,<sup>[14, 15]</sup> using a Diels-Alder (DA) / aromatization sequence. A similar strategy has been reported, using pinacol<sup>[16]</sup> or limonene as other bio-based platforms.<sup>[17]</sup> While mainly *para*-substituted aromatics are obtained from lignin, *ortho*- and *meta*-substituted aromatics can be

obtained from sugars and pinacol, further demonstrating the potential of biomass for the synthesis of aromatics.

Considering the current low price of fossil feedstocks, the production of bio-based aromatics with a higher value than BTX is a more reasonable approach. Functionalized aromatics such as benzaldehyde, benzylamine, benzonitrile, benzyl alcohol are typical examples with important applications in the field of fragrances, flavors, specialty polymers, agriculture, etc.

As mentioned above, renewable aromatics can be synthesized by reaction of bio-based furanic derivatives with olefins through a Diels-Alder/aromatization reaction. In this context, 5-hydroxymethylfurfural (HMF), “the sleeping giant” among sugar-derived chemicals, has received a growing interest, in particular for the synthesis of terephthalic acid. HMF is poorly reactive in the Diels-Alder (DA) reaction and is often reduced to 2,5-dimethylfuran<sup>[14]</sup> or oxidized to furan dicarboxylic esters<sup>[15]</sup> before undergoing a DA reaction. Although valuable aromatics were produced in high yields from HMF, the lack of cost-competitive processing technologies to convert low cost sugars to HMF currently hampers the industrial deployment of these routes. Note that BASF, Avantium and Avabiochem have recently communicated on the production of HMF at a pilot scale, indicating that mature technologies may be available in a close future for such application.

In contrast to HMF, furfural is a low cost furanic derivative (1-2€/kg) nowadays industrially produced in large scale from biomass waste (> 300 kT/year).<sup>[18]</sup> Like HMF however, furfural is poorly reactive in DA reactions. The electron withdrawing -CHO group reduces the nucleophilicity of the furanic ring (as shown by a severe lowering of the highest occupied molecular orbital (HOMO) energy vs. the parent furan), thus making the DA reaction unfavourable.<sup>[5]</sup> To circumvent this problem, furfural can be decarbonylated to furan before the DA reaction.<sup>[6,7]</sup> For instance, Hubert reported the synthesis of toluene and benzene by co-feeding ethylene or propylene with furfural at 450-600°C in the presence of ZSM-5, with *in situ* decarbonylation of furfural.<sup>[6a]</sup> Alternatively, to preserve the chemical functionality of furfural while decreasing the HOMO-LUMO gap, furfural can be derivatized to amines,<sup>[8]</sup> acetals,<sup>[9]</sup> alcohols,<sup>[10]</sup> phenolic-type resins<sup>[11]</sup> or amides,<sup>[12]</sup> making the DA reaction thermodynamically favorable. This strategy was employed to synthesize furfural-derived polymers which can be depolymerized *via* a retro-DA reaction at the end of life. The aromatization of these furfural-

derived cycloadducts has been investigated only sporadically. In 2016, Hailes reported the DA reaction of furfural dimethylhydrazone with highly activated dienophiles such as *N*-alkyl-maleimides at 80°C in water, followed by aromatization to the corresponding phthalimide derivatives.<sup>[13]</sup> However, starting from cheaper and more readily available olefins such as acrylonitrile or dimethyl maleate, the reaction yields were drastically lower (< 25% yield). Guided by DFT calculations, we recently reported the synthesis of *meta*-xylylenediamine (MXD), an important target in polymer chemistry, from furfural and acrylonitrile, two cheap and abundant chemicals.<sup>[5]</sup> Furfural was first derivatized with ethylene glycol, restoring the nucleophilicity of the furanic ring (upshift of the HOMO by 0.4 eV compared to furfural), and allowing the DA cycloadducts to be obtained with a yield of 75%. In addition, our strategy improved upon previous work in that (i) the subsequent aromatization step was catalyzed at low temperature (30°C) by bases, thus avoiding the competition with the retro-DA, and (ii) the reaction could be selectively driven to *meta*-substituted aromatics only, by playing with the rate of the aromatization reaction. Although this route was an expedient protocol to synthesize renewable MXD, predicting and controlling the *ortho* : *meta* selectivity during the Diels-Alder reaction remains highly desirable to widen the scope of this protocol for the synthesis of renewable aromatics.

The present work addresses this fundamental scientific challenge. Through a combined experimental-theoretical approach, we rationalize the impact of the substituents on furfural-derived diene and various dienophiles on the *ortho* : *meta* selectivity of the Diels-Alder reaction. Further, we present an improved protocol to aromatize the so-obtained Diels-Alder adducts to aromatics.

## Results and Discussion

### Reaction between 2-(furan-2-yl)-1,3-dioxolane and acrylonitrile.

As described in our previous report,<sup>[5]</sup> furfural was first converted to 2-(furan-2-yl)-1,3-dioxolane by reaction with ethylene glycol in the presence of a catalytic amount of Amberlyst-15. Next, the as-obtained 2-(furan-2-yl)-1,3-dioxolane was reacted with a 5-fold excess of acrylonitrile at 80°C, affording the corresponding DA cycloadducts (mixture of *ortho* and *meta* regioisomers, and corresponding *endo* and *exo* stereoisomers) in a combined yield of

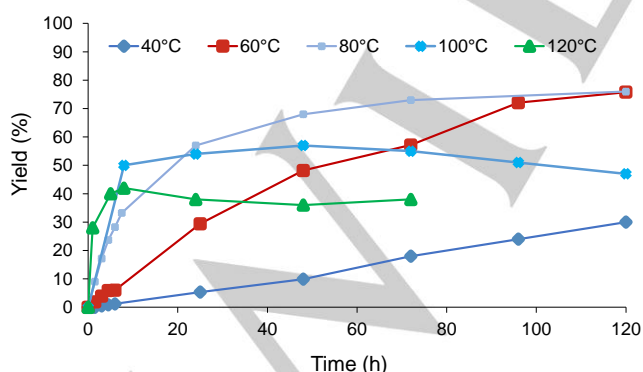


Figure 1. Total yield of DA cycloadducts as a function of time for the reaction of 2-(furan-2-yl)-1,3-dioxolane with a 5-fold excess of acrylonitrile at different temperatures.

73%, after 72 h of reaction (Fig. 1). The selectivity to the DA cycloadducts was 98%, the missing 2% corresponding to the deprotection of 2-(furan-2-yl)-1,3-dioxolane to furfural and ethylene glycol, presumably due to traces of water (stabilizer) in acrylonitrile (0.2-0.5% w/w). Extending the reaction time to 120 h resulted in a minor change of the yield (76%), indicating that the reaction had reached the DA vs. retro-DA equilibrium (Fig. 1).

### Selectivity of the Diels-Alder reaction.

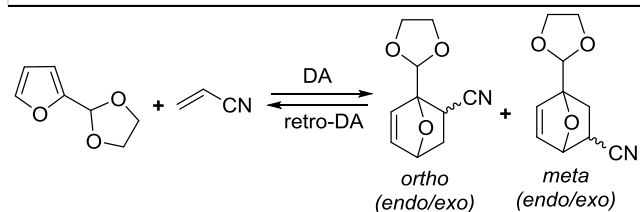
At equilibrium (measured after 120 h, see Fig. S1), the *ortho* : *meta* ratio reached a value of 52 : 48. After 120 h, the *endo* to *exo* ratios were 70 : 30 and 60 : 40 for the *ortho* and *meta* isomers, respectively. These features are captured reasonably well by DFT calculations (Tables S10-S11). First, activation barriers are in all cases (*ortho* or *meta*, *exo* or *endo*) found in a narrow energy range, ca 31.4-32.5 kcal/mol in free enthalpy. Thus, little to no kinetic selectivity is expected. Similarly, reaction free enthalpies range from +3.7 to +4.6 kcal/mol, suggesting low thermodynamic selectivity. Using a Maxwell-Boltzmann statistical model on relative reaction free enthalpies affords an *ortho* : *meta* ratio of 50 : 50 at 60°C, in line with experiments. Calculated *endo* : *exo* ratios are 67 : 33 and 46 : 54 for the *ortho* and *meta* isomers, respectively, again in good agreement with experiment.

These findings suggests that DFT calculations can be used to predict not only the feasibility but also the selectivity of DA reactions, which will provide very helpful throughout this work. Before going further, it is important to mention that from a practical perspective we are interested in *ortho* : *meta* ratios. Indeed, the *endo* : *exo* selectivity is lost in the aromatization step, while the *ortho* : *meta* selectivity is preserved. Therefore, in what follows, we will only discuss *ortho* : *meta* ratios; additional experimental and theoretical data on the *endo* : *exo* ratios is provided in the SI.

### Effect of the reaction temperature.

Increasing the reaction temperature from 80 to 100 and 120°C resulted in a much faster reaction, expressed as the time to reach the highest achievable (equilibrium) DA yield, but yields were lower with 52% after 24 h, and 42% after 8 h, at 100 and 120°C, respectively (Table 1, entries 1-3; Fig. 1). This means that at temperatures higher than 80°C, the retro-DA clearly became the dominating reaction. Conversely, a decrease of the temperature to 60°C resulted in a slower reaction but the maximum yield of the DA cycloadduct was identical to that obtained at 80°C (76%, Table 1, entry 4; Fig. 1). A further decrease of the reaction temperature to 40°C was possible but decreased the reaction rate to an unacceptable level (Table 1, entry 5; Fig. 1).

After ca. 24 h the *ortho* : *meta* ratio stabilized at ~50 : 50 for reaction temperatures of 40-60°C, decreasing to ~40 : 60 at 80-120°C, suggesting that the *meta* product is thermally slightly more stable than the *ortho* (Fig. S1). This trend is reproduced by DFT calculations, as temperature-dependent endergonic corrections from electronic energies to free enthalpies are slightly smaller for *meta* products than for *ortho* products (Table S11).

**Table 1.** Effect of the reaction temperature (entries 1-5) and dienophile to diene molar ratio (entries 6-8) on the DA reaction of 2-(furan-2-yl)-1,3-dioxolane with acrylonitrile.

Entry	Temp. (°C)	Acrylonitrile / 2-(furan-2-yl)-1,3-dioxolane ratio	Time (h) <sup>[a]</sup>	Yield (%) <sup>[b,c]</sup>
1	80	5	72 <sup>[a]</sup>	76
2	100	5	24 <sup>[a]</sup>	52
3	120	5	8 <sup>[a]</sup>	42
4	60	5	120 <sup>[a]</sup>	76
5	40	5	120 <sup>[a]</sup>	30
6	60	5	48	48 <sup>[d]</sup>
7	60	20	48	44 <sup>[d]</sup>
8	60	1	48	24 <sup>[d]</sup>

[a] time to reach maximum (equilibrium) yield; [b] maximum (equilibrium) yield; [c] other detected product (2%) are furfural and ethylene glycol; [d] not at reaction equilibrium, reactions were stopped after 48 h.

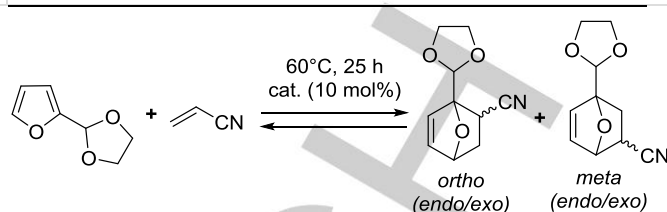
#### Effect of the dienophile to diene molar ratio.

Reactions were performed at 60°C and stopped after 48 h to assess the effect of the dienophile : diene molar ratio on the reaction rate. Increasing the acrylonitrile / 2-(furan-2-yl)-1,3-dioxolane molar ratio from 5 to 20 : 1 had no effect. However, a decrease from 5 to 1 slowed down the reaction, with only half the yield obtained after 48 h (Table 1, entries 6-8, Fig.S2). For practical reasons (the boiling point of acrylonitrile is 77°C), a temperature of 60°C was selected in the following experiments, together with an acrylonitrile : 2-(furan-2-yl)-1,3-dioxolane molar ratio of 5 : 1.

#### Effect of the catalyst.

Without catalyst, the DA reaction is quite slow at 60°C (Fig.1). For instance, after 25 h of reaction, the DA cycloadducts were obtained in only 26 % yield (Table 2, entry 1). To increase the formation rate of the DA cycloadducts, different Lewis acid catalysts (10 mol%), mostly metal chlorides, were screened (at 60 °C). The choice for Lewis acid catalysts was motivated by the fact that Brønsted acid catalysts led to tar-like materials as major products. In all cases, anhydrous Lewis acid catalysts were tested to limit the deprotection of 2-(furan-2-yl)-1,3-dioxolane to furfural and ethylene glycol.

Metal chlorides (MCl<sub>n</sub> with M = Ga, In, Sc, Cu, Hf and Nb) led to the formation of unidentified black soluble and insoluble materials as main product (Table 2, entries 2-7). With M = Mn, Cd, Sr, Bi, Sn, Li and Al, the reaction took place, but no improvement of the yield was observed after 25 h of reaction, compared to catalyst-free conditions (Table 2, entries 8-14). Even worse, these metal

**Table 2.** Effect of Lewis acid catalysts on the DA reaction of 2-(furan-2-yl)-1,3-dioxolane with acrylonitrile.<sup>[a]</sup>

Entry	Catalyst	DA cycloadduct yield (%)	Deprotection (furfural yield) (%)
1	-	29	2
2 <sup>[b]</sup>	GaCl <sub>3</sub>	-	-
3 <sup>[b]</sup>	ScCl <sub>3</sub>	-	-
4 <sup>[b]</sup>	InCl <sub>3</sub>	-	-
5 <sup>[b]</sup>	CuCl <sub>2</sub>	-	-
6 <sup>[b]</sup>	HfCl <sub>4</sub>	-	-
7 <sup>[b]</sup>	NbCl <sub>5</sub>	-	-
8	MnCl <sub>2</sub>	20	39
9	CdCl <sub>2</sub>	23	25
10	SrCl <sub>2</sub>	23	4
11	BiCl <sub>3</sub>	29	15
12	SnCl <sub>2</sub>	21	34
13	AlCl <sub>3</sub>	18	38
14	LiCl	26	15
15	CoCl <sub>2</sub>	51	10
16	ZnCl <sub>2</sub>	68	11
17	Zn(OTf) <sub>2</sub>	57	23
18	ZnI <sub>2</sub>	75	12
19	ZnI <sub>2</sub> /dppe	21	1
20	ZnI <sub>2</sub> /dmpe	23	1

[a] acrylonitrile/2-(furan-2-yl)-1,3-dioxolane molar ratio = 5; [b] tar-like materials were formed as major products.

chlorides catalyzed the concomitant deprotection of 2-(furan-2-yl)-1,3-dioxolane (4-39% yield) with moisture from the air atmosphere and/or water contained in acrylonitrile (0.2-0.5% w/w). In contrast, in the presence of Co or Zn chloride, significantly higher yields of 51 and 68 %, respectively, were reached after 25 h (and 75% after 48 h of reaction, Fig. S3, Table 2, entries 15-16). Unlike with the other metal chlorides, the deprotection of 2-(furan-2-yl)-1,3-dioxolane was limited (~10% yield), although it was still higher than under catalyst-free conditions (2%). To explore the effect of the counter anion, Zn(OTf)<sub>2</sub> and ZnI<sub>2</sub> were also screened, affording the DA cycloadducts in 57 and 75% yield, respectively,

after 25 h (Table 2, entries 17-18). The low yield obtained with  $\text{Zn}(\text{OTf})_2$  is probably due to its high hygroscopicity, promoting in turn deprotection to furfural (23%, Table 2, entry 17).  $\text{ZnI}_2$  was found to be the most efficient catalyst screened, as further confirmed by a kinetic profile which showed that the equilibrium yield was reached slightly earlier than with  $\text{ZnCl}_2$  (Fig. S3). Addition of strong complexing agents such as 1,2-bis(diphenylphosphino)ethane (DPPE) or 1,2-bis(dimethylphosphino)ethane (DMPE) to  $\text{ZnI}_2$  or  $\text{ZnCl}_2$  inhibited their catalytic activities, further confirming the catalytic role of these Lewis acids (Table 2, entries 19-20). Finally, it should be noted that the *ortho* : *meta* ratio was not significantly affected by the presence of the catalyst (Fig. S4). For the remainder of the study,  $\text{ZnCl}_2$  was preferred over  $\text{ZnI}_2$ , because it is cheaper and it does not lead to yellow coloration of the reaction products, while its catalytic activity is very similar to that of  $\text{ZnI}_2$ .

#### Effect of the protective group on furfural.

Different protective agents were used to derivatize furfural, with the aim of assessing the effects on yield and isomer ratio. To this end, furfural was reacted with different diols, amino-alcohols and also 1,2-ethanedithiol (see SI for details of synthesis and characterization). The as-obtained furfural derivatives were reacted with acrylonitrile under the same conditions as 2-(furan-2-yl)-1,3-dioxolane, *i.e.* 60°C, 10 mol%  $\text{ZnCl}_2$ , and 5 equiv. of acrylonitrile (Table 3, entries 1-5). The reaction with 2-(furan-2-yl)-1,3-dioxolane is shown for comparison in entry 1. Additional experiments were also carried out in the absence of catalysts (Table S3). DFT calculations suggested the feasibility of all these reactions with HOMO-LUMO gaps similar to those found for the successful combination of 2-(furan-2-yl)-1,3-dioxolane with acrylonitrile (6.89-7.39 eV, Table S3).

**Table 3.** Reaction of acetal and thioacetal derivatives of furfural with acrylonitrile.

$\text{X} = \text{O}, \text{S}$

Entry	Diene	Yield (%)	Experimental <i>ortho</i> : <i>meta</i> ratio (%)	Calculated <i>ortho:meta</i> ratio (%) <sup>[c]</sup>	
				Thermodynamic selectivity <sup>[d]</sup>	Kinetic selectivity <sup>[e]</sup>
1 <sup>[a]</sup>		75	50 : 50	50 : 50	63 : 37
2 <sup>[b]</sup>		81	53 : 47	55 : 45	58 : 42
3 <sup>[b]</sup>		85	52 : 48	56 : 44	59 : 41
4 <sup>[a]</sup>		68	43 : 57	43 : 57	57 : 43
5 <sup>[a]</sup>		67 73 <sup>[f]</sup>	39 : 61 91 : 9	37 : 63	90 : 10

[a] Reaction time = 48 h; [b] reaction time = 25 h; [c] based on a Maxwell-Boltzmann statistical model using DFT-calculated energies (see SI for details); [d] based on relative free enthalpies of reaction at 60°C; [e] based on relative free enthalpies of activation at 60°C; [f] reaction temperature = 30 °C.



As expected from the DFT predictions, these furfural derivatives underwent reaction in all cases (Table 3, entries 1-5). The yields at equilibrium were similar to what was found for 2-(furan-2-yl)-1,3-dioxolane (67-85%, Table 3, entries 2,5). The selectivity to the DA cycloadducts always exceeded 89% (95% without  $\text{ZnCl}_2$ ), with furfural and the protecting agent being formed as the only side products (by deprotection of the furfural derivate). Note, that using amino alcohols (ethanol amine, *N*-methylethanolamine) as derivatizing agents of furfural led to an unexpected reaction outcome (Table S3). Instead of forming DA adducts, the starting oxazolidine-derived furfural was converted, but a complex mixture of unidentified products was formed, tentatively attributed by NMR spectroscopy to uncontrolled Michael-type reaction with acrylonitrile.

At equilibrium, the *ortho* : *meta* ratio of DA adducts was around 50 : 50 for all alcohol-protected furfural derivatives (Table 3, entries 1-4), albeit with a slightly higher amount of the *meta* isomer in the case of 2-(furan-2-yl)-4,4,5,5-tetramethyl-1,3-dioxolane (pinacol derivative) (Table 3, entry 4). For the thiol-derivative 2-(1,3-dithiolan-2-yl) furan, an even higher amount of *meta* isomer was observed (Table 3, entry 5). Note, that in the absence of a catalyst, similar trends were observed (Table S3). The experimental product ratios are in excellent agreement with equilibrium product ratios obtained from DFT-calculated relative free enthalpies of reaction (Table 3, entries 1<sup>a</sup>-5<sup>d</sup>, and Tables S10-S19), confirming that the thermodynamic equilibrium had been reached in all cases. In contrast, poorer agreement is found with ratios calculated from DFT-calculated relative free enthalpies of activation, representing kinetic conditions.

We now turn our attention to isomer ratios at the beginning of the reaction, where such kinetic selectivity should manifest. Noteworthy, both with and without catalyst, the *ortho* DA cycloadduct is initially formed in a higher amount than the *meta* adduct (Table S3, Fig. S6). This effect is most evident for 2-

(furan-2-yl)-4,4,5,5-tetramethyl-1,3-dioxolane and 2-(1,3-dithiolan-2-yl) furan, with initial amounts of *ortho* adduct of 65% and 74%, respectively, at 30-40% conversion (Table S3). When the reaction time is extended, the *ortho* : *meta* ratios converge to the values obtained at the reaction equilibrium (Table S3, Fig. S6), strongly suggesting that the *ortho* adduct is the kinetic product. DFT modelling, based on activation free enthalpies at 60°C, nicely reproduces these observations with a kinetic selectivity for the *ortho* adduct, markedly more pronounced for 2-(1,3-dithiolan-2-yl) furan. To support this hypothesis, we carried out the reaction of 2-(1,3-dithiolan-2-yl) furan at 30°C in the presence of  $\text{ZnCl}_2$ . As expected, under these conditions, the *ortho* DA cycloadduct was the major product (91%, see Table 3, entry 5). Note that, due to the lower temperature, leading to inhibition of the retro-DA reaction, the yield slightly increased from 67 to 73%, (Table 3, entry 5, Figs. S5 and S6). The experimental and calculated endo : exo ratios were, within experimental or computational error, identical for the *meta* isomer of all DA adducts, showing a slight preference for the endo isomer. This preference was more pronounced in the case of the *ortho* isomer, Table S4). Again, a similar trend was observed in the absence of catalyst, although the reaction equilibrium had not been reached yet (Table S3).

#### Reaction of 2-(furan-2-yl)-1,3-dioxolane with other dienophiles.

Since the DA reaction of 2-(furan-2-yl)-1,3-dioxolane and acrylonitrile had been successful, other relevant dienophiles were also tested, *i.e.* acrolein, methyl vinyl ketone, and methyl acrylate. The calculated HOMO-LUMO gaps for the combination of these dienophiles with 2-(furan-2-yl)-1,3-dioxolane (6.89-7.47 eV, Table S5) were comparable to that found for the combination with acrylonitrile ( $\Delta E = 7.39$  eV), suggesting that these reactions

**Table 4.** Reaction of 2-(furan-2-yl)-1,3-dioxolane with different dienophiles.<sup>[a]</sup>

Entry	-R	Yield (%) <sup>[b]</sup>	Experimental <i>ortho</i> : <i>meta</i> ratio (%) <sup>[b]</sup>	Calculated <i>ortho</i> : <i>meta</i> ratio (%) <sup>[c]</sup>	Experimental <i>ortho</i> : <i>meta</i> ratio (%) < 15 % conv.	Calculated kinetic <i>ortho</i> : <i>meta</i> ratio (%) <sup>[d]</sup>
1	-CN	76	48 : 52	50 : 50	48 : 52	63:37
2	-COCH <sub>3</sub>	36	13 : 87	14 : 86	41 : 59	19:81
3	-COOCH <sub>3</sub>	40	33 : 67	18 : 82	44 : 56	48:52
4	-CHO	28	38 : 62	28 : 72	47 : 53	31:69
5	-CH <sub>2</sub> NH <sub>2</sub>	-	-	-	-	-

[a] Dienophile / 2-(furan-2-yl)-1,3-dioxolane molar ratio = 5; [b] at equilibrium; [c] based on a Maxwell-Boltzmann statistical model (see SI for details), using DFT-calculated relative free enthalpies of reaction at 60°C; [d] based on relative free enthalpies of activation.

should be feasible as well. Indeed, the reactions were successful (carried out without catalyst, see Fig. S7 for kinetic profiles).

At equilibrium, the DA reaction plateaued at 28-40% yield with methyl acrylate, methyl vinyl ketone, and acrolein compared to 75% with acrylonitrile (Table 4 and Fig. S7). The selectivity of the reaction remained close to 100%, suggesting that the retro-DA reaction was less favorable for acrylonitrile than for the other dienophiles. We also tested allyl amine as an example of an electron-rich dienophile. The HOMO-LUMO gap calculated by DFT was high (9.24 eV), indicating that the DA should not proceed, as indeed observed experimentally. This result shows that only electron poor dienophiles are eligible for DA reaction with 2-(furan-2-yl)-1,3-dioxolane.

The nature of the dienophile also impacts the *ortho* : *meta* ratio. Although in all cases the *ortho* cycloadduct was the kinetic product, at equilibrium the *meta* product was predominant (Table 4 and Fig. S8), in particular in the case of methyl vinyl ketone, with 87% *meta* isomer (Table 4, entry 2). Again, the experimental findings are well reproduced by DFT calculations, with a clear thermodynamic *meta* selectivity for methyl vinyl ketone, methylacrylate and acrolein with an *ortho* : *meta* ratios of 14:86, 18:82 and 28:72, respectively, using free enthalpies of reaction (Table 4, entries 2-4, and Tables S20-S32). As observed earlier, for all *ortho* and *meta* isomers, a slight preference for the *endo* isomer was observed, both experimentally and theoretically (Table S5).

### Reaction of other furanic dienes with acrylonitrile.

To assess the molecular diversity of DA cycloadducts that could be obtained through this pathway, other-furfural-derived dienes such as 2-furionitrile, furfuryl amine, furfuryl alcohol, ethylfurfuryl ether, and 2-methylfuran, nowadays obtained on a large scale from furfural, were screened. Like furfural, 2-furionitrile contains an electron-withdrawing substituent (the –CN group), and consequently the HOMO-LUMO gap calculated by DFT ( $\Delta E = 7.77$  eV) suggested an unreactive combination (for comparison,  $\Delta E = 7.72$  eV for the unsuccessful combination of furfural and acrylonitrile). In contrast, the other furfural derivatives contain an electron-donating group which should permit the reaction with acrylonitrile, as corroborated by HOMO-LUMO gaps (6.94-7.09 eV, Table S6), comparable to the reactive combination of 2-(furan-2-yl)-1,3-dioxolane and acrylonitrile ( $\Delta E = 7.39$  eV).

Consistent with the prediction from DFT, no DA reaction was observed for 2-furionitrile, while it was successful for furfuryl alcohol, ethyl furfuryl ether and 2-methyl furan, with equilibrium yields of 81%, 54% and 69%, respectively (Table 5). In the case of furfuryl amine (Table 5, entry 2), a mixture of different products was obtained, due to concomitant Michael addition of the –NH<sub>2</sub> group on acrylonitrile. The DA cycloadduct was observed by NMR (again consistent with the prediction from DFT) but, due to significant formation of side products, it was not possible to accurately determine the corresponding yield by <sup>1</sup>H NMR. Noteworthy, in the case of 2-furionitrile, attempts to perform an inverse electron demanding DA reaction by reaction with allyl amine also failed (HOMO-LUMO gap = 7.94 eV).

**Table 5.** Reaction of furan derivatives with acrylonitrile.

Entry	-R	$\Delta E(\text{HOMO-LUMO})$ (eV)	Yield (%)	Experimental <i>ortho</i> : <i>meta</i> ratio (%) at equilibrium	Calculated thermodynamic <i>ortho</i> : <i>meta</i> ratio (%) <sup>[a]</sup>	Experimental <i>ortho</i> : <i>meta</i> ratio (%) at 15 % conv.	Calculated kinetic <i>ortho</i> : <i>meta</i> ratio (%) <sup>[b]</sup>
1	-CN	7.77	-	-	-	-	-
2	-CH <sub>2</sub> NH <sub>2</sub>	7.09	n.d. <sup>[c]</sup>	-	-	-	-
3	-CH <sub>2</sub> OH	7.03	81	60 : 40	57 : 43	72 : 28	82 : 18
4 <sup>[d]</sup>	-CH <sub>2</sub> OEt	7.04	54	64 : 36	63 : 37 <sup>[e]</sup>	66 : 34	81 : 19 <sup>[e]</sup>
5	-CH <sub>3</sub>	6.94	69	66 : 34	61 : 39	85 : 15	91 : 9

[a] based on a Maxwell-Boltzmann statistical model (see SI for details), using DFT-calculated relative free enthalpies of reaction at 60°C; [b] based on relative free enthalpies of activation; [c] n.d. means not determined, furfuryl amine successfully reacted with acrylonitrile but a complex mixture of compounds was obtained due to parasite Michael addition of furfuryl amine to acrylonitrile, making impossible the determination of the reaction yield; [d] the reaction was stopped after 48 h because extending the reaction produced tar-like material; [e] the calculations were performed on a simplified model (ethyl group replaced by methyl).

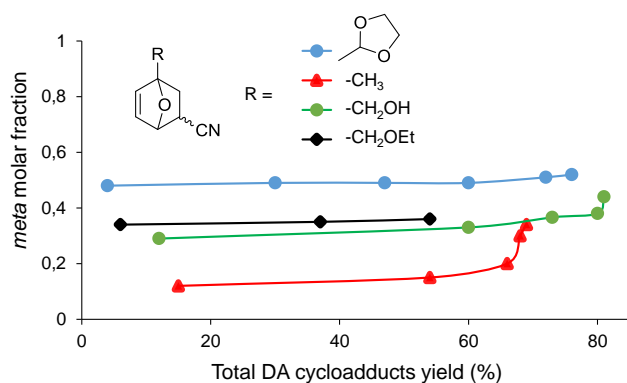


Figure 2. Effect of the substitution of the furanic ring on the *ortho* : *meta* ratio. Acrylonitrile : derivatized furfural molar ratio = 5, reaction temperature = 60°C, without catalyst.

At equilibrium, the *ortho* : *meta* ratio varied from 60 : 40 to 66 : 34, with 2-methyl furan showing the highest *ortho* selectivity (Table 5, entries 3-5), higher than in all other cases explored so far. Kinetic profiles (Fig. 2, Fig. S9) show that the *ortho* DA cycloadduct is the kinetic product, like in all other cases. At < 15% conversion, the *ortho* DA was formed in different amounts: 2-methylfuran (85%), furfuryl alcohol (72%), ethylfurfuryl ether (66%) and 2-(furan-2-yl)-1,3-dioxolane (52%), indicating that substituents on the furanic ring also impact the initial formation rate of the *ortho* and *meta* DA cycloadducts (Fig. 2, Fig. S9). DFT calculations once again nicely retrieve the experimental findings, both in terms of thermodynamic and kinetic selectivity (Table 5, entries 3-5, Tables S33-S40). Again, for all DA cycloadducts, the *endo* isomers were formed preferentially (Table S6).

#### Optimal combination of diene and dienophile.

Again guided by HOMO-LUMO gaps determined by DFT calculations (Table S7), furfuryl alcohol, ethylfurfuryl ether and 2-methylfuran were next reacted with different dienophiles (acrolein, methyl vinyl ketone and methyl acrylate) to further improve molecular diversity and to further assess how substituents impact the yield and *ortho* or *meta* selectivity. As suggested by DFT

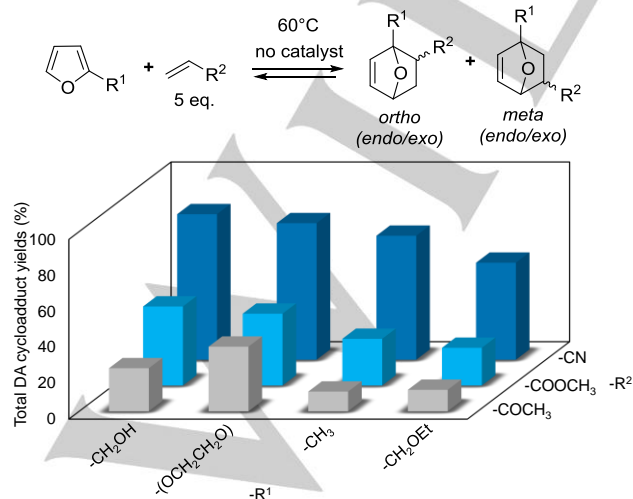


Figure 3. Combination of various furfural-derived chemicals and dienophiles. Dienophile : derivatized furfural molar ratio = 5 : 1, reaction time = 120 h (except for the combination of acrylonitrile with ethylfurfuryl ether for which the reaction time was 48 h).

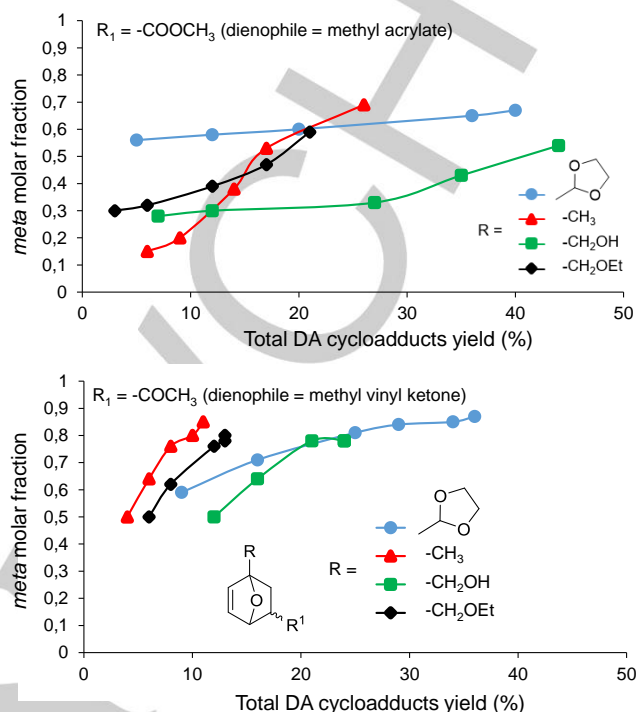


Figure 4. *ortho* : *meta* molar fraction as a function of the combined yield of DA cycloadducts, using methyl acrylate and methyl vinyl ketone as dienophiles. Dienophile : diene molar ratio = 5, reaction temperature = 60°C.

calculations, all tested combinations were successful, affording a library of DA cycloadducts with different chemical functionality (Fig. 3). As found with 2-(furan-2-yl)-1,3-dioxolane, the highest equilibrium yields of DA cycloadducts were obtained using acrylonitrile as a dienophile, confirming again that the -CN group has the strongest promoting effect on the yield of the DA cycloadduct.

In line with what was discussed earlier for the combination of methyl vinyl ketone with 2-(furan-2-yl)-1,3-dioxolane (Table 4), at equilibrium, the amount of *meta* DA cycloadducts was the highest with methyl vinyl ketone (87%), followed by methyl acrylate (67%), indicating that the *ortho* : *meta* ratio was mostly governed by the substituent present on the dienophile. As observed for acrylonitrile, the *ortho* cycloadduct was always the kinetic product (Fig. 4).

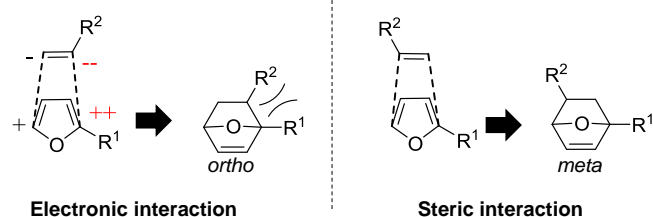
#### Elements of rationalization.

As we have seen, DFT calculations proved successful in reproducing the experimental *ortho* : *meta* selectivity, both under kinetic and thermodynamic conditions. But beyond the reproduction and prediction of data, modelling offers insight into the fundamentals of this selectivity. Chemical intuition suggests that *meta* addition should minimize the steric repulsion between the pending group of the diene ( $R_1$ ) and the pending group of the dienophile ( $R_2$ ), as well as the deformation energy required to reach the transition state and product geometries. On the other hand, in the spirit of the Klopman-Salem model of reactivity,<sup>[19]</sup>



charge control would result in the interaction of the most charged sites of both reagents (Scheme 1). Natural population analysis (NPA)<sup>[20]</sup> shows that the two carbon atoms of the diene carry positive partial charges with different relative magnitude (+ and ++), depending on the substituent  $R_1$ , while the two carbon atoms of the dienophile carry negative partial charges (- and --), again differing in magnitude, depending on the substituent  $R_2$ .

The highest partial charges on both diene and dienophile are always found on the carbon atoms linked to the respective substituents (Table S8). In the DA reaction, the coulombic interaction between the reaction partners is maximized when the most charged atoms interact, *i.e.* the most positive partial charge on the diene will attract the most negative partial charge on the dienophile. Hence, the functional groups of the resulting DA adduct end up in an *ortho* arrangement (Scheme 1).



Scheme 1. Competition between electronic and steric interactions: ++ / + and - / - indicate the relative magnitude of the positive and negative partial charges of the carbon atoms involved in bond formation during the DA reaction.

For the reaction of a given dienophile with different dienes, the higher the charge difference ( $\delta$ ) between the pro-*ortho* and pro-*meta* C atoms of the diene, the higher is the expected *ortho* selectivity (and by definition the lower is the *meta* selectivity). This is indeed the case, with a reasonable correlation between  $\delta$  and the experimental *ortho* : *meta* ratio at equilibrium found in the reaction of acrylonitrile with different furfural derivatives (Figure 5).

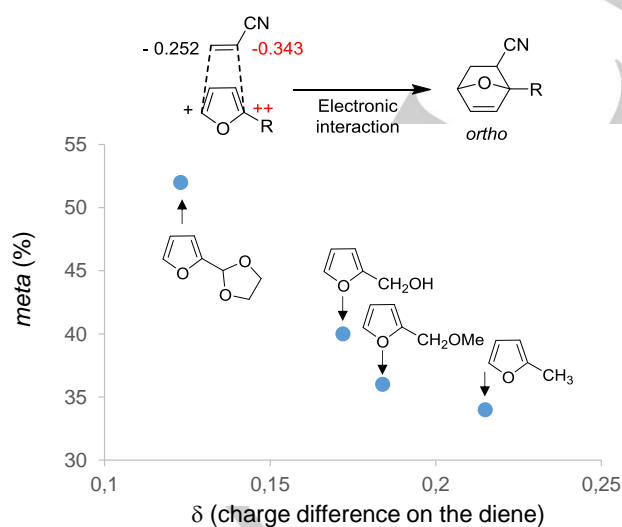


Figure 5. Experimental equilibrium *meta* selectivity as a function of the calculated charge difference ( $\delta$ ) between the two C atoms of the double bond of the diene, for the reaction of acrylonitrile with different dienes.

In the same spirit, for the reaction of a given diene with different dienophiles, the charge difference between the two olefinic carbons on the dienophile should impact the selectivity: for methyl vinyl ketone (trans isomer:  $\delta = 0.009$  e) methyl acrylate (trans isomer:  $\delta = 0.036$  e) and acrolein (trans isomer:  $\delta = 0.049$  e) is significantly lower than that of acrylonitrile ( $\delta = 0.091$  e) (Fig. 6,

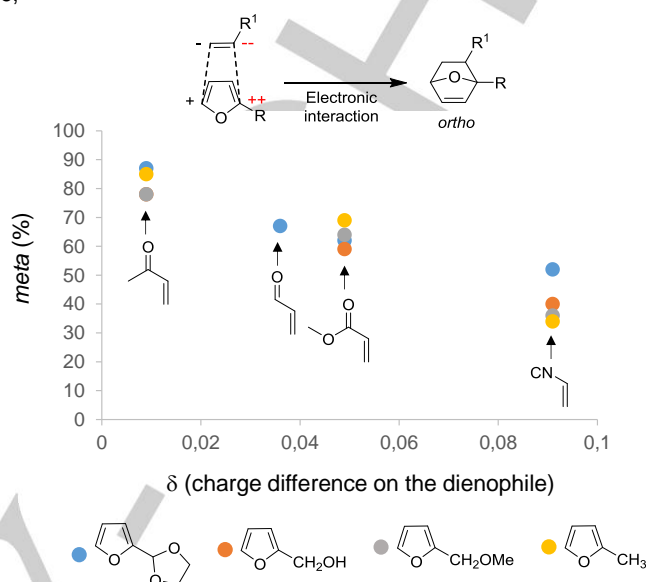


Figure 6. Experimental equilibrium *meta* selectivity as a function of the charge difference ( $\delta$ ) between the two C atoms of the double bond of the dienophile for various combinations of dienophiles and dienes. For the sake of clarity, only the *trans* isomer of the respective dienophile is represented. See SI for more information on the *cis* isomer (Table S8).

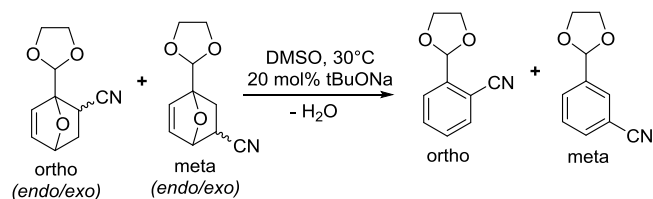
Table S8). Hence, the difference in electronic interaction between furfural-derived chemicals and these dienophiles is expected to be lower than with acrylonitrile, and formation of the *ortho* cycloadduct should be less favored. This claim is supported by Figure 6 showing that, irrespective of the starting diene, the lower the  $\delta$  on the dienophile, the higher the amount of *meta* product. Note, that while steric effects cannot be properly quantified here, it is reasonable to assume that such effects now take over, thus favoring the formation of the *meta* product.

To summarize, we may propose a “rule of thumb” to account for the experimental observations: here, the observed selectivity stems from a competition between steric interaction, favoring *meta* addition, and electronic interactions, favoring *ortho* addition (Scheme 1). The model also has the additional benefit that it can be used by non-experts. Instead of time-consuming explicit calculations of reaction pathways, only partial charges of the reactants are necessary, acting as convenient descriptors for selectivity.

#### Aromatization reaction

As previously reported by us, the DA cycloadducts derived from furfural can be quantitatively aromatized, with the loss of water, in the presence of a catalytic amount of sodium *tert*-butoxide and at only 30°C, thus preventing the unwanted competitive retro-DA reaction.<sup>[5]</sup> This protocol relies on DMSO as a solvent in order to produce *in situ* a superbases, by solvation of sodium by DMSO.<sup>[21]</sup> We found here that, except in the case of 2-(1,3-

dithiolan-2-yl) furan for which no aromatization was observed, for all other tested protective agents, the aromatization reaction proceeded well (70-80% yield), always with the *meta* aromatic being formed more rapidly than the *ortho* isomers (Fig. S10, Table S9), a mean to produce consecutively, but separately, the *ortho* and *meta* aromatics, as previously shown by us.<sup>[5]</sup>



Scheme 2. Base-catalyzed aromatization of the DA cycloadducts.

Although this protocol is an expedient way to produce various functionalized renewable aromatics in nearly quantitative yields, the use of DMSO as a solvent may raise ecological issues. However, since the role of DMSO is to solvate *t*BuONa, we surmised that it should be possible to use it in a small amount (as a co-solvent). In what follows, the aromatization of the DA cycloadducts obtained from 2-(furan-2-yl)-1,3-dioxolane and acrylonitrile was selected as a case study (Scheme 2). DMSO was first employed as a co-solvent with toluene. In a mixture of DMSO and toluene, the aromatization was observed, but the yields of aromatics were lower than in pure DMSO; 42% and 10% in a mixture DMSO/toluene 1/1 and 1/3, respectively (vs 90% in neat DMSO) (Table 6, entries 2,3). These results can be explained by the inhibition of the DMSO/ *t*BuONa superbase by released water. Indeed, in neat DMSO, the initial production rate of aromatics ( $r_{\text{aromatic}}$ ) was 1.83 mmol/h (Fig. 7). However, when 5 eq. of water (relative to the DA cycloadduct) were initially added into DMSO,  $r_{\text{aromatic}}$  decreased to 0.42 mmol/h and the aromatization reaction stopped at 57% conversion. A further incremental increase of the initial amount of water in DMSO from 5 to 10 and 20 eq. stopped the reaction at yield of only 48% and 29%, respectively, and further decreased the aromatization rate to 0.18 and 0.05 mmol/h, respectively, reflecting the deactivation of the DMSO/ *t*BuONa superbase by water.

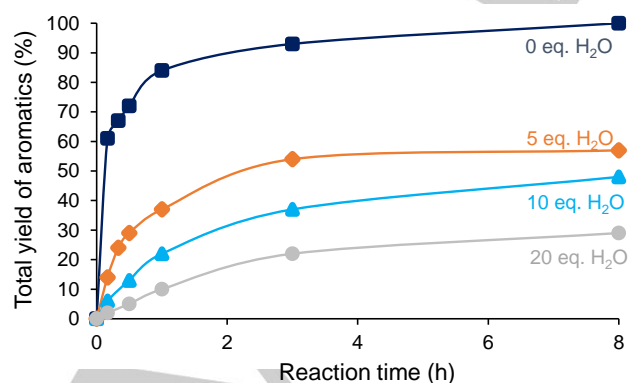


Figure 7. Effect of water on the total yield of aromatics (30°C, DMSO, 20 mol % *t*BuONa).

To maintain the catalytic activity of the DMSO / *t*BuONa superbase while limiting its deactivation by released water, the aromatization reaction was therefore conducted under reflux in toluene, in a Dean-Stark apparatus, and in the presence of only 2.5% of DMSO. Pleasingly, with continuous removal of water, aromatics were formed in 81% yield after only 10 min of reaction. Here again, the *meta* aromatic was always produced faster than the *ortho* isomer (Table 6, entry 4).

**Table 6.** Influence of solvents on the base-catalyzed aromatization of the DA cycloadduct obtained from 2-(furan-2-yl)-1,3-dioxolane and acrylonitrile.

Entry	Solvent	Total yield of aromatics (%)	<i>ortho</i> : <i>meta</i> ratio (%)
1	DMSO	93	30 : 70
2	DMSO/Toluene (1/1)	42	9 : 91
3	DMSO/Toluene (1/3)	10	5 : 95
4	Toluene + 2.5% DMSO	81	50 : 50

## Conclusion

We show that the Diels-Alder reaction of cheap alkenes with industrially available bio-based furfural and its derivatives is a promising pathway for the synthesis of functionalized renewable aromatics. Various furfural-derived dienes were successfully coupled at 60°C to various dienophiles featuring electron-withdrawing groups (-CHO, -CN, -COCH<sub>3</sub>, -COOCH<sub>3</sub>), affording the corresponding DA cycloadducts with yields ranging from 28 to 85% at the thermodynamic equilibrium. In all cases, the DA reaction proceeds with a selectivity higher than 98%. The reaction can be accelerated by ZnCl<sub>2</sub> or ZnI<sub>2</sub> catalysts, while maintaining the reaction selectivity higher than 90%. Pleasingly, it is possible to control the *ortho* : *meta* ratio by a suitable choice of the substituents on diene and dienophile and the reaction conditions (kinetic or thermodynamic). The *ortho* product is the kinetic product, in the sense that it forms faster than the *meta* adduct. Conversely, under thermodynamic conditions, the *meta* product is more stable in most cases.

DFT calculations were carried out to not only predict the feasibility of the DA reaction for the different diene and dienophile combinations, but also to understand how the *ortho* : *meta* ratio depends on the substituents on the dienes and dienophiles. We find excellent agreement between experimental and calculated product ratios under both thermodynamic and kinetic conditions, underlining the value of DFT calculations as predictive tool for organic chemistry and biomass valorization. We find that the substituents on the dienes and dienophiles impact the reaction outcome in two principal ways. First, the (thermodynamic) feasibility of the reaction is conditioned by the HOMO-LUMO gap between the reactants, which in turn depends on the electron-withdrawing or -donating nature of the substituents. The calculated HOMO-LUMO gap can thus be used as a convenient descriptor for the feasibility of the reaction. Second, the *ortho* : *meta* selectivity of the reaction depends on the balance between steric repulsion, favoring the *meta* isomers, and electronic interactions (characterized by charges), orienting towards the *ortho* products. As a result, the highest selectivity to the *ortho* isomer is obtained for the reaction of acrylonitrile and methyl furan, while the highest *meta* selectivity is observed with

methyl vinyl ketone, independent of the furan derivative. The calculated charges of the reactants thus allow a quick estimation of the *ortho* : *meta* selectivity, as alternative to the calculation of full reaction pathways.

This work also points to an optimization of the aromatization step. Notably, by continuous removal of released water, it was possible to perform the base-catalyzed aromatization reaction in a toluene/DMSO (97.5:2.5 mass ratio) mixture, instead of neat DMSO as previously described by us.

By providing efficient synthetic and predictive tools to overcome the low reactivity of bio-based furfural in Diels-Alder reaction, we do believe this work complements the scope of biomass for the supply of renewable aromatics. While *para*-substituted aromatics are mainly produced from lignin, the present work opens the door to *ortho*- and *meta*-substituted aromatics from sugar-derived furfural.

## Experimental Section

**General procedure for Diels-Alder reaction:** 50 mmol of furan derivative was mixed with 250 mmol of a dienophile and heated under N<sub>2</sub> atmosphere at 60°C for 25–48 h in a carousel flask equipped with a magnetic stirring bar and a condenser. At the DA equilibrium, the excess of dienophile was removed by distillation under vacuum. The as-recovered DA cycloadduct can be directly used as collected for the subsequent aromatization reaction. For characterization purposes the DA cycloadduct was purified by flash chromatography (silica gel, EtOAc/cyclohexane).

Catalytic Diels-Alder reactions were performed in a similar way, with the addition of 0.1 eq. of catalyst, preferentially ZnCl<sub>2</sub> or ZnI<sub>2</sub>. In such case, the catalyst needs to be removed (by purification over silica gel) before engaging the DA cycloadduct in the aromatization step.

**Aromatization reaction:** The reaction was performed as described in our previous work.<sup>[5]</sup>

**Computational details:** All calculations were performed using Gaussian 16 rev B, at the M06-2X/6-311++G(d,p) level of theory. The M06-2X functional indeed provides reliable reaction paths for Diels Alder additions, both in terms of selectivity and reactivity,<sup>[22]</sup> while inclusion of polarization and diffuse functions was shown to be necessary in the calculation of sulphur-containing compounds.<sup>[23]</sup>

All geometries were fully optimized and frequency calculations were performed in order to confirm the nature of the stationary points. Unless stated otherwise, all calculations used an implicit solvation model (PCM), with a dielectric constant of  $\epsilon = 33.0$  (25°C, 1 bar value for acrylonitrile). HOMO-LUMO energy values were extracted from the last single point evaluation on the optimization calculations. *Endo/exo* selectivity were evaluated for both *ortho* and *meta* attacks on the dienophile, and two conformers of the diene were considered (conformation of the furan substituting group on position 2). This led to 8 transition state and 8 product structures in the case of acrylonitrile. For the other dienophiles (methyl acrylate, acrolein, methyl vinyl ketone), additional geometries were considered because of the *cis/trans* isomerism around the conjugated bond, resulting in 16 transition state and 16 product structures. Atomic charges were calculated for the optimized structures, using the Natural Population Analysis method as implemented in NBO version 3.1 for Gaussian. The computed natural charges for the reagents are provided in Table S8.

## Acknowledgements

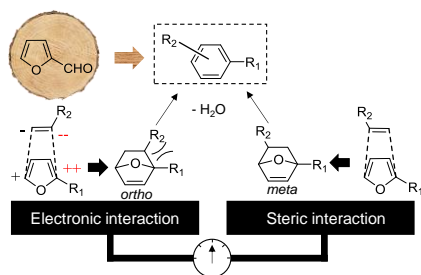
The authors are grateful to the CNRS, the University of Poitiers, the Région Nouvelle Aquitaine, and SOLVAY for financial support. The International Consortium on Eco-conception and Renewable Resources (FR CNRS INCREASE 3707) and the chair “TECHNOGREEN” are also acknowledged for their funding?

**Keywords:** Aromatics • Bio-based furanics • Diels-Alder • DFT • Renewables

- [1] <https://www.lelementarium.fr/product/benzene-toluene-xylenes/>; consulted on March 21<sup>st</sup> 2019.
- [2] a) <http://publications.lib.chalmers.se/records/fulltext/185085/185085.pdf>, consulted on March 21<sup>st</sup>, 2019; b) A. Maneffa, P. Priece, J. A. Lopez-Sanchez, *ChemSusChem* **2016**, 9(19), 2736–2748; c) H. D. Embree, T. H. Chen, G. F. Payne, *Chem. Eng. J.* **2001**, 84(2), 133–147.
- [3] a) T. Renders, S. Van den Bosch, S. F. Koelewijn, W. Schutyser, B. F. Sels, *Energy Environ. Sci.* **2017**, 10, 1551–1557; b) Y. Huang, Y. Duan, S. Qiu, M. Wang, C. Ju, H. Cao, Y. Fang, T. Tan, *Sustainable Energy Fuels* **2018**, 2, 637–647; c) E. M. Anderson, M. L. Stone, R. Katahira, M. Reed, G. T. Beckham, Y. Román-Leshkov, *Joule* **2017**, 1, 613–622; d) R. Rinaldi, R. T. Woodward, P. Ferrini, H. J. E. Rivera, *J. Braz. Chem. Soc.* **2019**, 30(3), 479–491; e) T. Renders, G. Van den Bossche, T. Vangeel, K. Van Aelst, B. Sels, *Curr. Opin. Biotechnol.* **2018**, 56, 193–201.
- [4] a) A. Arbentz, L. Avérous, *Green Chem.* **2015**, 17, 2626–2646; b) L. Roumeas, G. Billerach, C. Aouf, E. Dubreucq, H. Fulcrand, *ACS Sust. Chem. Eng.* **2018**, 6 (1), 1112–1120; c) L. Roumeas, C. Aouf, E. Dubreucq, H. Fulcrand, *Green Chem.* **2013**, 15(11), 3268–3275; d) A. Zhang, J. Li, S. Zhang, Y. Mu, W. Zhang, J. Li, *RSC Adv.* **2017**, 7(56), 35135–35146.
- [5] I. Scodeller, S. Mansouri, D. Morvan, E. Muller, K. De Oliveira Vigier, R. Wischert, F. Jérôme, *Angew. Chem.* **2018**, 130(33), 10670–10674; *Angew. Chem. Int. Ed.* **2018**, 57(33), 10510–10514.
- [6] a) Y. Cheng, G. W. Huber, *Green Chem.* **2012**, 14, 3114–3125; b) A. E. Settle, L. Berstis, N. A. Rorrer, Y. Roman-Leshkov, G. T. Beckham, R. M. Richards, D. R. Vardon, *Green Chem.* **2017**, 19, 3468–3492.
- [7] Y. Tachibana, S. Kimura, K. Kasuya, *Sci. Rep.* **2015**, 5, 8249.
- [8] C. Garcia-Astrain, A. Gandini, D. Coelho, I. Mondragon, A. Retegi, A. Eceiza, M. A. Corcuera, N. Gabilondo, *Eur. Polym. J.* **2013**, 49, 3998–4007.
- [9] a) N. Teramoto, M. Niwa, M. Shibata, *Materials* **2010**, 3, 369–385; b) H. Satoh, A. Mineshima, T. Nakamura, N. Teramoto, M. Shibata, *React. Funct. Polym.* **2014**, 76, 49–56; c) S. Takano, F. Ito, K. Ogasawara, *Pharm. Soc. Jpn.* **1982**, 102(2), 153–161; d) N. Teramoto, Y. Arai, M. Shibata, *Carbohydr. Polym.* **2006**, 64, 78–84; e) K. Fischer, S. J. Hünig, *J. Org. Chem.* **1987**, 52, 564–569; f) A. Guidi, V. Theurillat-Moritz, P. Vogel, *Tetrahedron* **1996**, 7(11), 3153–3162.
- [10] Y. Bai, M. De Bruyn, J. H. Clark, J. R. Dodson, T. J. Farmer, M. Honoré, I. D. V. Ingram, M. Naguib, A. C. Whitwood, M. North, *Green Chem.* **2016**, 18, 3945–3948.
- [11] G. Çayli, S. Kusefoglu, *J. Appl. Polym. Sci.* **2011**, 120, 1707–1712.
- [12] a) J. A. Mikroyannidis, *Appl. Polym. Sci. A Polym. Chem.* **1992**, 30, 125–132; b) M. Oikawa, M. Ikoma, M.; Sasaki, *Tet. Lett.* **2005**, 46, 415–418; c) F. I. Zubkov, I. K. Airiyani, J. D. Ershova, T. R. Galeev, V. P. Zaytsev, E. V. Nikitina, A. V. Varlamov, *RSC Adv.* **2012**, 2, 4103–4109.
- [13] S. Higson, F. Subrizi, T. D. Sheppard, H.C. Hailles, *Green Chem.* **2016**, 18, 1855–1858.
- [14] a) J. C. Kim, T. W. Kim, Y. Kim, R. Ryoo, S. Y. Jeong, C. U. Kim, *Appl. Catal. B Env.* **2017**, 206, 490–500; b) R. Y. Rohling, E. Uslamin, B. Zijlstra, I. C. Tranca, I. A. W. Filot, E. J. M. Hensen, E. A. Pidko, *ACS Catal.* **2018**, 8, 760–769; c) Y. P. Wijaya, D. J. Suh, J. Jae, *Catal. Commun.* **2015**, 70, 12–16; d) Y. P. Wijaya, H. P. Winoto, Y. Park, D. J. Suh, H. Lee, J. Ha, J. Jae, *Catal. Today* **2017**, 293–294, 167–175; e) C. L. Williams, C. C. Chang, P. Do, N. Nikbin, S. Caratzoulas, D. G. Vlachos, R. F. Lobo, W. Fan, P. J. Dauenhauer, *ACS Catal.* **2012**, 2, 935–939; f) C. C. Chang, S. K. Green, C. L. Williams, P. J. Dauenhauer,

- W. Fan, *Green Chem.* **2014**, *16*, 585-588; g) D. Wang, C. M. Osmundsen, E. Taarning, J. A. Dumesic, *ChemCatChem* **2013**, *5*, 2044-2050; h) I. F. Teixeira, B. T. W. Lo, P. Kostetsky, M. Stamatakis, L. Ye, C. C. Tang, G. Mpourmpakis, S. C. E. Tsang, *Angew. Chem.* **2016**, *128*(42), 13255-13260; *Angew. Chem. Int. Ed.* **2016**, *55*, 13061-13066; i) M. Shiramizu, F. D. Toste, *Chem. Eur. J.* **2011**, *17*, 12452-12457; j) J. M. Fraile, J. I. Garcia, M. A. Gomez, A. de la Hoz, J. A. Mayoral, A. Moreno, P. Prieto, L. Salvatella, E. Vasquez, *Eur. J. Org. Chem.* **2001**, *15*, 2891-2899; k) X. Ding, S. T. Nguyen, J. D. Williams, N. P. Peet, *Tet. Lett.* **2014**, *55*, 7002-7006.
- [15] a) J. J. Pacheco, M. E. Davis, *Proc. Nat. Acad. Sci. USA.* **2014**, *111*, 83636-8367; b) J. J. Pacheco, J. A. Labinger, A. L. Sessions, M. E. Davis, *ACS Catal.* **2015**, *5*, 5904-5913; c) M. Orazov, M. E. Davis, *Chem. Sci.* **2016**, *7*, 2264-2274.
- [16] a) Y. Hu, N. Li, G. Li, A. Wang, Y. Cong, X. Wang, T. Zhang, *Green Chem.* **2017**, *19*, 1663-1667; b) Y. Hu, N. Li, G. Li, A. Wang, Y. Cong, X. Wang, T. Zhang, *ChemSusChem* **2017**, *10*, 2880-2885.
- [17] M. Colonna, C. Berti, M. Fiorini, E. Binassi, M. Mazzacurati, M. Vanini, S. Karanam, *Green Chem.* **2011**, *13*, 2543-2548.
- [18] a) R. Mariscal, P. Maireles-Torres, M. Ojeda, I. Sádaba, M. López Granados, *Energy Environ. Sci.* **2016**, *9*, 1144-1189; b) X. Li, P. Jia, T. Wang, *ACS Catal.* **2016**, *6*(11), 7621-7640.
- [19] a) L. Salem, *J. Am. Chem. Soc.* **1968**, *90*, 543-552; b) G. Klopman, *J. Am. Chem. Soc.* **1968**, *90*, 223-234.
- [20] a) A. E. Reed, F. Weinhold, *J. Chem. Phys.* **1983**, *78*, 4066-4073; b) A. E. Reed, R. B. Weinstock, F. Weinhold, *J. Chem. Phys.* **1985**, *83*, 735-746.
- [21] B. A. Trofimov, *Sulfur Reports* **1992**, *11*(2), 207-231
- [22] D. Yepes, J. Valenzuela, J. I. Martínez-Aray, P. Pérez, P. Jaque, *Phys. Chem. Chem. Phys.* **2019**, *21*, 7412-7428.
- [23] W. M. Wah, Quantum Chemical Calculations of Sulfur-Rich Compounds in *Elemental Sulfur and Sulfur-Rich Compounds II; Elemental sulfur and sulfur-rich compounds*; **2003**, Springer

## Entry for the Table of Contents



We report here the synthesis of renewable aromatics from bio-based furfural and various alkenes, using a Diels-Alder/aromatization sequence. This investigation aims at rationalizing, and even predicting, not only the feasibility of the Diels-Alder reaction but also the effect of substituents on the *ortho* : *meta* selectivity.